TUTORIAL REVIEW

CSR
www.rsc.org/csr

Low temperature single crystal X-ray diffraction: advantages, instrumentation and applications

A. E. Goeta* and J. A. K. Howard
Durham University, Department of Chemistry, Durham, UK DH1 3LE.
E-mail: A.E.Goeta@durham.ac.uk

Received 2nd March 2004
First published as an Advance Article on the web 17th September 2004

The benefits of carrying out single crystal X-ray diffraction (SXRD) experiments at low temperatures have long been recognised by the scientific community, as clearly demonstrated by the massive increase in publications reporting the use of low temperature SXRD in the past 15 years. This *tutorial review* will summarise the advantages, many of them now often forgotten by its practitioners or never known by the newcomers to the field, of performing single crystal X-ray diffraction experiments at low temperatures. The instrumentation currently available to university laboratories, which has been greatly improved over the past 5 years, will also be briefly described and a few different examples covering a range of applications will be presented.

Andrés Goeta is a Senior Research Officer at the University of Durham (since 1998). He obtained his Licenciatura and Doctorate physics degrees from the University of La Plata (Argentina). His PhD work involved the study of electrostatic properties of materials of pharmacological interest, through the study of their electron density. In 1993, he was awarded a British Chevening Scholarship by The British Council, to work at the University of Durham. Since then, his work has concentrated on the structural study of new materials by low temperature diffraction methods and the subsequent correlation to their physical properties.

A. E. Goeta

Judith Howard is the Professor of Structural Chemistry at the University of Durham, a position she has held since 1991. Her research interests embrace X-ray and neutron crystallography at low temperatures and under pressure and include high-resolution charge density studies. After working at Oxford for her D.Phil. degree with Dorothy Hodgkin O.M., she was appointed to the staff at Bristol University, where she established a significant crystallography group within the Inorganic Chemistry Department of F. G. A. Stone. She has gained several awards, including a CBE for 'services to science', the RSC Prize for Structural Chemistry (1998), an EPSRC Senior Fellowship (1998–2003) and was elected Fellow of The Royal Society in 2002.

J. A. K. Howard

Introduction

Most modern characterisation techniques used in chemistry yield information either on the presence and connectivity of certain chemical groups, or on specific aspects of the chemical or physical properties of a compound. In contrast, crystallography is the only technique that enables the acquisition of full detailed structural information, including the relative position of atoms as well as their motion in the solid state. Since the chemical and physical properties of a material *de facto* depend on its structure, this information is essential and consequently crystallography has become one of the most valuable characterisation techniques available to the modern chemist.

Within the realm of crystallography (the study of crystalline matter by diffraction techniques), single crystal X-ray diffraction (SXRD) is by far the most commonly used technique available for the determination of the crystal and molecular structure of crystalline solids. Other techniques available involve the use of neutron diffraction or electron diffraction and studies can be performed on crystalline powders as well as single crystals. Each of these methods is invaluable in its own right, however, in this review we are going to concentrate on SXRD. This technique is essentially very simple: a single crystal scatters a collimated, monochromatic beam of X-rays, and the scattered beams diffracted by the sample are then measured. Processing information about the position and intensity of these diffracted X-ray beams (or reflections) yields information about the atomic arrangement within the crystalline material. However, modern crystallography is not only about knowing the positions of the atoms and corresponding bond distances, angles and related features within a material. The far more important and interesting aspect of this technique is the correlation of structural features with physical properties. This can include optical, magnetic and conductive effects as well as the structural behaviour under external stimulus or in different chemical environments. The resulting knowledge increases our understanding of the complex, underlying processes, ultimately aiding the design of new materials in which the desired chemical or physical properties are enhanced. From this point of view, the control of the sample's external environment during data collection is vitally important and one of the most basic environmental variables that can be tuned to the user's requirements is the crystal temperature. Altering the temperature of a crystal will change its behaviour and therefore, its

DOI: 10.1039/b312763j

chemical and physical properties in a number of ways, which will be outlined herein. More specifically we will focus on the effects of cooling a crystal below room temperature, since the practice of carrying out SXRD experiments at low temperatures has become common practice in university laboratories around the world.

The increase in the availability of low temperature crystallography has come about not only as a result of the number and variety of currently marketed cooling devices, but also because it is generally accepted that structural information obtained in this way is of better quality than that obtained at room temperature. The massive increase in publications reporting the use of low temperature SXRD from 1978 to 2002 can be seen in Fig. 1, from information obtained from the Cambridge

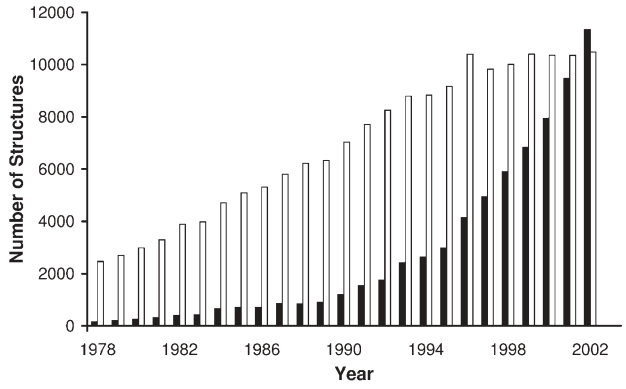

Fig. 1 CSD search comparing the number of laboratory single crystal X-ray structure determinations carried out between 1978 and 2002 at room temperature (283 K $\leqslant T \leqslant$ 303 K, shown in white) and the number of those carried out below 283 K (shown in black).

Structural Database (Version 5.25, January 2004).[1] Within this period, the percentage of structures determined by single crystal X-ray diffraction below 283 K has risen from only 6% to 52%. However, despite having become a standard procedure, with benefits long recognised by the scientific community,[2,3] more and more students, as well as young scientific researchers, are using low temperature SXRD without a full comprehension of the consequences and advantages of its use. For this reason, we hope that this tutorial review will serve those many starting practitioners as a first point of contact with the subject.

Consequences and advantages of using low temperature for diffraction experiments

Reduction or suppression of the radiation damage

The structural information sought in an X-ray diffraction experiment is usually that of the original unperturbed crystalline material. However, it has been long known that the interaction of X-rays with a crystal lattice often results in irreversible damage to a crystal.[4] This is usually observable by following the steady decline in intensity of some standard reflections, measured during the course of the data collection. Initial concern about this phenomenon and its influence on the accurate measurement of integrated intensities led to a survey of the effects of radiation damage to single crystals.[5] In spite of the small number of materials reported therein, the results pointed to a dependence of the radiation damage on the intensity of the X-rays used for the experiment, *i.e.* certain reflections from compounds studied with Cu radiation showed a greater decline in intensity than those studied with Mo radiation.† Subsequently, Seiler and Dunitz[7] discussed the effects of radiation in organic crystals. They found that the intensity loss due to radiation damage not only increases with exposure time, but also with increasing scattering angle. This latter effect is equivalent to an intensity fall-off due to an increase in temperature. In addition to this, they observed an increase in the mosaic spread, reflected in the widths of the reflection profiles. These observations suggested that the general effect of radiation damage in single crystals is a loss of long-range order and an increase in crystal defects, *i.e.* a loss of crystallinity.

The process of radiation damage is more important when measuring proteins rather than small molecules, mainly due to the longer data collection times required, but also due to the high content of water in proteins.[8] For this reason, the process of radiation damage has been studied more carefully with respect to X-ray diffraction data measurements carried out on proteins, and in particular for measurements performed with synchrotron radiation, due to the vastly increased doses of X-rays received by crystals in these cases.[9–11] These results reinforced the conclusions drawn previously by Seiler and Dunitz, who deduced that the damage results in a loss of resolution in the diffraction pattern and an increase in the mosaicity of the crystals.

It is now accepted that the mechanism for radiation damage can be divided into two stages.[11,12] The first stage involves immediate damage to molecules by the incident X-ray beam removing electrons from atoms, and thus generating radiolytic products. This effect is then dose dependent, increasing with X-ray flux, but also time dependent, as the total amount of X-ray photons received by a sample increases with time. The second stage involves these radiolytic products travelling through the crystal and damaging the lattice as they do so. This effect is then time dependent, but is also temperature dependent, as at higher temperatures, it is easier for these radicals to diffuse through the lattice. This diffusion will damage parts of the crystal which are not directly exposed to the beam and a good description of many different reactions taking place in a protein crystal after irradiation, is given by Burmeister.[13] It is then clear that lowering the temperature of a crystal during an X-ray diffraction experiment will reduce the radiation damage by immobilising or slowing down the diffusion through the lattice of these X-ray generated radicals.

Despite the general benefit that low temperature has on the samples used during diffraction experiments by reducing radiation damage, it has been shown by Larsen *et al.* that radiation damage can occur in crystals of small molecules at temperatures as low as 9 K, when the data collection times are unusually long (55 days in the case reported).[2] In general, for molecular crystals and laboratory X-ray sources, the combination of low temperature with currently much used area detectors and hence drastically reduced collection times, usually makes radiation damage negligible.

Reduction of the thermal motion

When using diffraction for the study of crystalline matter, the main interest and effect of reducing the temperature of the sample crystal is in the reduction of the lattice vibrations. This is due to the influence of the vibrations on the intensities of the Bragg reflections. These Bragg intensities, usually measured from a large number of diffracting planes with Miller indices

† Cu X-ray tubes produce a higher flux of photons than Mo due to a number of reasons including the probability that the decay of an excited state leads to the emission of a photon and absorption of the generated X-rays by the target itself.[6]

hkl, are proportional to the square of the amplitudes of the structure factors, F_{hkl}, which are defined as:

$$F_{hkl} = \sum_{i=1}^{n} f_i T_i \exp\left(2\pi i(hx_i + ky_i + Iz_i)\right) \quad (1)$$

where the summation is over all atoms in the unit cell (n), each one having a scattering power given by the X-ray scattering factor f_i and with fractional atomic coordinates x_i, y_i, z_i. The term T_i is called the temperature factor and it takes into account the thermal motion of each atom. Considering atoms that do not move is equivalent to having $T_i = 1$. For moving atoms $T_i < 1$, and so it is apparent that the temperature factor represents the reduction in scattering power due to the lattice vibrations, which are in turn dependent on the temperature of the crystal, and of course related to the atom type/size and its position in the molecule and unit cell.

In order to model how atoms move in a crystalline solid, we need to make certain assumptions about the forces between atoms, which of course need not be the same in all directions. The best known assumption, is called the harmonic approximation. Within this approximation, if an atom is displaced from its position, a force proportional to this atomic displacement will push it back towards its original position. Thus $F = -kx$. This force does not involve second, third or higher powers of the displacements, which implies a potential energy proportional to the square of the displacements ($V = kx^2$). Within the harmonic approximation, the temperature factor is given by the expression:

$$T_i = \exp\left(-\frac{1}{2}\langle (Q.u_i)^2 \rangle\right) \quad (2)$$

where Q is the scattering vector, u_i is the instantaneous displacement of atom i and the $<\ldots>$ brackets indicate a time-averaged value over a period of time much longer than the period of vibration of the individual atom. For isotropic atomic vibrations, the expression [2] becomes:

$$T_i = \exp\left(-\frac{8\pi^2 \sin^2\theta}{\lambda^2}\langle u_i^2 \rangle\right) = \exp\left(-\frac{8\pi^2 \sin^2\theta}{\lambda^2} U_{iso}\right) = \exp\left(-\frac{\sin^2\theta}{\lambda^2} B_{iso}\right) \quad (3)$$

where θ is the Bragg angle and λ is the radiation wavelength. $B_{iso} = 8\pi^2 U_{iso}$ is called the isotropic displacement parameter, while U_{iso}, the most commonly reported form of the displacement parameter represents the mean square amplitude of the displacement. In the case of different amplitudes of vibration in different directions, six parameters are used to model the atomic displacement, the anisotropic displacement parameters, U_{ij}. These parameters define an ellipsoid (*i.e.* its orientation with respect to the unit cell axes and the length of its principal axes), the size of which represents the probability of an atom being located within its boundaries.[14]

Observed data to higher 2θ angles. Due to a combined effect of the functional shapes of the atomic scattering factors and the atomic temperature factors, the observed Bragg intensities are reduced as the scattering angle increases. In the hypothetical case of all electrons being situated at one point, the atomic scattering factor of an atom will be equal to its atomic number Z. However, given that the dimensions of the finite volume occupied by the electrons of an atom are of the same order of magnitude as the wavelength of the X-rays, there will in general be a path difference between the X-rays scattered by different electrons in the same electron cloud. For $2\theta = 0$ the path difference is 0 and $f_i = Z$, but as 2θ increases the path difference will increase smoothly and the destructive

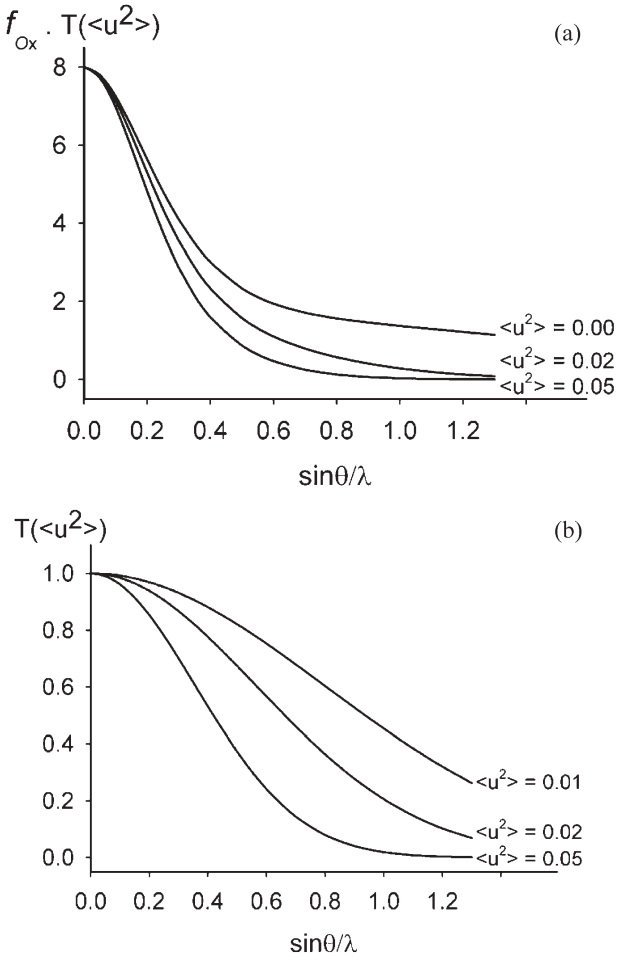

Fig. 2 (a) Scattering power of oxygen as a function of sinθ/λ after the convolution of its scattering factor with the temperature factor ($T(<u^2>) = \exp(-8\ \pi^2\ <u^2>\ \sin^2\theta/\lambda^2)$) for values of $<u^2> =$ 0.00, 0.02 and 0.05 Å^2. (b) Temperature factor *vs.* sinθ/λ for values of $<u^2> = 0.01$, 0.02 and 0.05 Å^2.

interference will also increase, making $f_i << Z$ at high 2θ angles.[14] Fig. 2(a) shows a plot of the theoretical scattering factor for oxygen as a function of sinθ/λ,[15] but obviously this scattering power could only be realised if the temperature was absolute zero ($T_i = 1$, $<u_i^2> = 0$). At higher temperatures, thermal motion produces an even larger smear of the electron density. Fig. 2(b) shows a plot of the temperature factor (eqn. [3]) as a function of sinθ/λ for several values of the mean square atomic displacement $<u_i^2>$ (typical values for oxygen atoms in molecular crystals vary from 0.01 to 0.05 Å^2 between 10 K and 300 K respectively). It is clear from this figure that the value of the temperature factor falls very fast for values of sinθ/λ above 0.2 Å^{-1}. The combination of the reduction in scattering power due to the shape of the scattering factor and the temperature factor is highlighted in Fig. 2(a), where the scattering factor for oxygen as a function of sinθ/λ, modified by typical values for the mean square atomic displacement in molecular crystals at room temperature ($<u_i^2> = 0.05$ Å^2) and at or below an approximate temperature of 120 K ($<u_i^2> = 0.02$ Å^2) are shown. It can be seen that at room temperature the oxygen atom will not scatter much beyond 0.7–0.8 Å^{-1}, while at temperatures below 120 K, it will scatter with the same power up to 1.0–1.1 Å^{-1}. Thus, by lowering the temperature of the crystal, there will be a larger contribution towards the total Bragg scattering of the crystal up to a higher resolution than at room temperature. In this way, it becomes meaningful to collect high resolution data at low temperatures, *i.e.* to collect data to higher values of sinθ/λ (or equivalently to

higher values of 2θ for a given wavelength), since in this case the data is not only measurable, but also contains valuable information about the atoms which produce such scattering.

Reduction of dynamic disorder and librational effects. The mean square atomic displacements extracted from diffraction data represent averages not only over space (since the structural information obtained for a unit cell is in truth the average of all unit cells in a far from perfect crystal), but also over time, as the time of a diffraction experiment is orders of magnitude larger than the periods of vibration. Performing experiments at different temperatures makes it possible to distinguish between possible static disorder and vibrational motion of the atoms. Lowering the temperature of the experiment will not change any static disorder within a crystal, but will significantly reduce any disorder due to atomic vibrations. For example, spherical anions such as BF_4^-, PF_6^-, ClO_4^-, *etc.*, are often badly disordered at room temperature as any orientation of the anion is energetically equivalent, unless the anion is locked into position by intermolecular contacts. However, they become more ordered as the temperature is reduced, and the atomic positions for these groups become much easier to model. Moreover, by reducing the thermal smear of the electron density, any static disorder will also be easier to model as the different 'components' of this disorder are easier to identify.

Librational effects, or atomic vibrations along an arc instead of a straight line, will produce artificially shortened bond lengths.[14] The model obtained from the diffraction experiment gives the distance between mean atomic positions, not the instantaneous separation between atoms. As such, the experiment can lead to artificially shorter distances than the true ones. However, these effects can also be minimised by reducing the temperature of the experiment, as the arc of oscillation becomes smaller and closer to a straight line (Fig. 3).

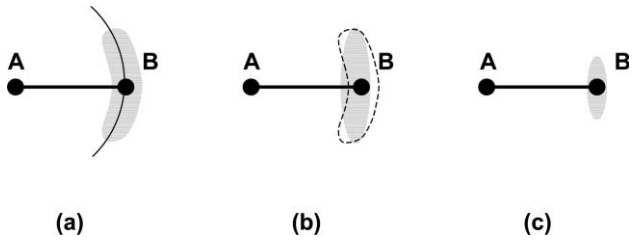

Fig. 3 Libration and its effects: (a) By keeping the A–B bond length constant, vibration of atom B around A is done in an arc (libration). (b) The electron density is modelled as an ellipsoid, producing artificial bond shortening. (c) Low temperature decreases this thermal motion, reducing the error.

Reduction of anharmonic effects. Although when modelling atomic temperature factors we normally work within the harmonic approximation (see above), this is not strictly true and sometimes the approximation may not be a valid one. Atoms can sit in asymmetric potential energy wells resulting in anharmonic motion, *i.e.* curvilinear atomic motion. In the harmonic approximation, the representational surface within which an atom has a certain probability of being found due to the thermal vibrations is an ellipsoid, because only quadratic terms in the displacement are included in the expression for the temperature factor. Anharmonic effects will introduce higher order terms needed to represent the true atomic motion, which will make the representational surface different from ellipsoidal (as in the case of librational effects). However, the anharmonicity is much smaller at the bottom of the potential energy well,

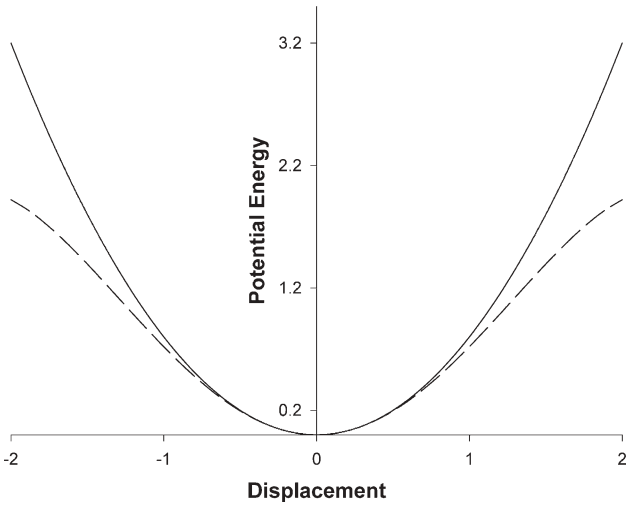

Fig. 4 Schematic representation of the potential energy wells for harmonic (solid line, $V = -ku^2$) and anharmonic (dashed line, $V = -ku^2 - k'u^4$, $k = k' = 0.08$) approximations.

hence lowering the temperature makes the harmonic approximation more valid (Fig. 4). In spite of this, in some cases anharmonic motion can still be present at liquid-nitrogen temperatures.[16]

Reduction of thermal diffuse scattering. It has been shown[17] that the intensity of X-rays scattered by a crystal is the sum of the elastically scattered (where there is no change in the energy/momentum of the X-ray photons) and inelastically scattered (where the X-ray photons suffer a change in energy) X-ray photons. The inelastic scattering arises from the interactions of the X-ray photons with one or more phonons (quantum mechanical 'particles' representing lattice vibrations). While the elastic scattering gives rise to the Bragg reflections, the intensity arising from the inelastic terms is called 'thermal diffuse scattering' (TDS).

TDS will be distributed throughout the whole of the reciprocal space, though unfortunately not uniformly. The inelastic one-phonon scattering (interaction of X-ray photons with one-phonon) due to the low frequency acoustic‡ modes is the highest contributor to the TDS and moreover, it shows up as peaks at the reciprocal lattice points, *i.e.* coinciding with the positions of the Bragg intensities (Fig. 5). The reason for this 'unfortunate' coincidence is that atomic motions in solids are not independent, but are in fact coupled together. Separating the Bragg scattering and one-phonon TDS contribution in a given reflection is not trivial. It requires a special correction, which needs knowledge of the elastic constants for the material at hand, and is dependent on the temperature of the experiment as well as the kind of scan used to measure the reflection and the Bragg angle θ of that reflection.[17]

The TDS that originates from the high frequency optic§ modes of vibration and/or from multi-phonon processes, on the other hand, fluctuates much more slowly in reciprocal space, and thus can be considered constant within the extent of a Bragg reflection (Fig. 5). In this way, most of this form of TDS is eliminated from the Bragg intensities during data reduction when performing the background subtraction.

Obviously, thermal diffuse scattering is a function of the thermal motion of the atoms and so it will decrease when the

‡ The name 'acoustic' arises because at the limit of long wavelengths, the frequencies of these modes tend to zero and behave like waves in an elastic medium.

§ The name 'optic' arises because of the strong coupling of these modes with dipole electromagnetic radiation.

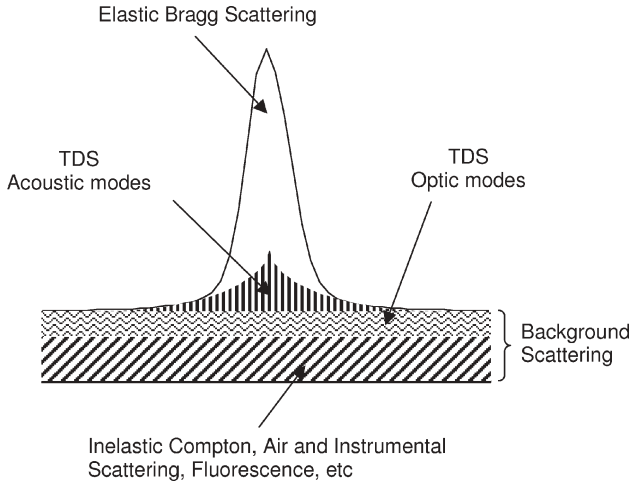

Fig. 5 Representation of the X-ray scattering around a Bragg peak, highlighting the contributions arising from different effects.

temperature is lowered, as reducing the temperature will de-excite and reduce the effect of the lattice vibrations. TDS is also larger for materials with low elastic constants, like molecular compounds, and it increases at high scattering angle. When the amount of TDS is considerable and no correction is or can be performed on the data, the atomic displacement parameters appear artificially small.[18] For most molecular compounds the elastic constants are not known, and so a correction is not possible. For this reason, it is highly advantageous to perform the diffraction experiment at the lowest possible temperature if accurate Bragg intensities are required. For example, Iversen *et al.*[19] calculated correction factors for magnesium showing how, at 298 K, the TDS contribution to the observed diffraction amounts to $\sim$20% of the intensity of reflections at $\sin\theta/\lambda = 0.8$ Å^{-1}. However, this value reduces to $\sim$8% at 125 K and no correction was deemed necessary for data collected at 8 K.

Instrumentation

A variety of cooling techniques and numerous types of cooling equipment have been used to study the low temperature properties of materials.[20,21] However, for laboratory crystallographic studies, one method dominates, the nitrogen gas-stream method, with which temperatures down to 80 K are obtainable. For attaining lower temperatures, a variety of helium based liquid and gas cryostats are available.

Open flow nitrogen gas cryostats

Within this first method, it should be safe to say that the most known and widely used cryostat is the Oxford Cryosystems Cryostream (Fig. 6).[22] In this and other similar systems, liquid nitrogen in an unpressurised Dewar vessel is pumped through a vacuum insulated pipe into a high-vacuum insulated chamber. Here, the liquid is evaporated and the resulting gas warms up while passing a heat exchanger. Subsequently the gas is recooled by the liquid nitrogen while passing back through the heat exchanger before escaping through the delivery nozzle onto the sample. A heating coil and thermal sensor located in the delivery nozzle regulates and controls the final gas temperature.

A very convenient feature of this kind of cryostat is the fact that the sample can be seen at all times during the experiments, allowing relatively easy control over other possible external features of the experiment, *e.g.* experiments under an electric field,[23] light irradiation of the sample,[24,25] *in situ* crystallisation of liquids and gases,[26] flash-freezing of a sample mounted in an

Fig. 6 Bruker SMART-1K CCD area detector diffractometer equipped with both an Oxford Cryosystems Cryostream N_2 and Helix He open flow gas cryostats for low temperature measurements. In addition, a laser is permanently mounted on the goniometer for the measurement of light induced excited states.

oil drop,[27,28] *etc.* Care must be taken when using this kind of system as it is possible to find a temperature difference between that of the sample and the one reported by the thermal sensor in the nozzle. Careful calibration, monitoring and adjustment of the distance from the sample to the nozzle usually prevents this problem.

Open flow nitrogen gas cryostats are now a very common feature of a modern crystallography laboratory. Hundreds of them are working all around the world, and it is now very rare to acquire a new SXRD instrument without the accompanying N_2 cryostat.

Helium based cryostats

A natural extension to the nitrogen gas cryostat is to use helium instead of nitrogen,[29–31] allowing temperatures of less than 15 K. The main drawback of such an instrument is the availability and cost of liquid helium, which is boiled to produce the cold stream of helium gas used for cooling the sample. To keep the costs of the cryogen under budget, liquid helium flow cryostats could be used[32] where liquid helium is boiled by direct contact with a copper block on which the sample crystal is mounted. In such a system, a cryogen recovery system could make it economically viable.

However, closed-cycle helium refrigerators (CCR) are historically more important and have also been used in university laboratories, although due to their cost and difficult maintenance, only very few of these instruments are currently running.[33–36] In these, a compressor unit pressurizes the helium gas for the expander, where refrigeration is accomplished by adiabatic expansion of the helium gas, which is in thermal contact with the sample. The main advantages of CCRs are the low temperatures attainable, $\sim$10 K, the fact that they do not consume cryogen, and the good agreement between the temperature of the sample and that of the thermal sensor. Further advances in this area are now being marketed, offering minimum temperatures of 1.8 K,[37] but to our knowledge

none have been installed in a university laboratory to date. The key disadvantage of CCR systems however, is that the crystal is not visible during the experiment, since it is mounted inside two or three concentric cylindrical beryllium shrouds that are evacuated for thermal insulation.

Now, to combine the advantages of the two techniques described above, a natural extension of these two approaches would be a combination of them, *i.e.* an open flow helium gas cryostat. The advantages are the same as those of the nitrogen gas stream cryocoolers and the two main limitations with this kind of cooling device are the cost of helium gas and the prevention of frosting. However, a very successful device of this kind has been on the market for the past 5 years, allowing crystallographic measurements down to 30 K.[24,25,38–40]

In this method, bottled helium gas is cooled by passing it through heat exchangers mounted on a two stage, closed-cycle He refrigerator. The cold He gas finally escapes into the atmosphere through a specially designed nozzle and onto the sample. A turbomolecular vacuum pump is used to continuously pump the space around the cryostat's internal components to minimise unwanted heat leaks into the system. A standard, large, high pressure gas cylinder lasts approximately 24 hours, and switching gas bottles in order to provide a continuous supply of helium gas is possible without affecting the sample temperature, thus enabling long term experiments to be performed. A second outer helium gas stream at room temperature provides shielding for the cold stream, thus helping to avoid thermal contact between the cold stream and the atmosphere, reducing icing problems. A small beryllium shield tube extends from the nozzle around and beyond the crystal to keep the flow of helium laminar and hence protect the cold stream from atmospheric contamination. Notches within the walls of this beryllium tube prevent primary X-ray beam diffraction from the beryllium.

This kind of cryostat can be mounted on modern and nowadays common CCD area detector diffractometers (Fig. 6), allowing fast data collections and bringing the cost of the helium gas into the range of other consumable items. In addition, this helium cryostat has just been redesigned to allow the use of nitrogen gas as well as helium, avoiding the need to switch between cryostats, saving on cryogen costs while performing experiments above and below 80 K.[41]

Applications

There are a wide variety of applications of low temperature SXRD in studies of correlations between structure and property, and it is impossible to present examples of all of them here. Despite this, we would like to describe a few simple applications arising from the use of the technique in small molecule crystallography, followed by a few examples in which the use of low temperature is essential to the outcome of the investigation at hand.

Even when the aim of the experiment is only to determine the crystal and molecular structure of a crystalline material, which in principle could be done at room temperature, it is obvious from the consequences arising from the reduction of thermal motion mentioned above, that the use of low temperatures will allow more precise and accurate crystal structure analyses to be performed. As stated above, the increase in intensity gained by lowering the temperature of the experiment enables the collection of more valuable data, increasing the number of reflections per refined parameter. In addition, by increasing their intensity, these reflections are better measured because the peak intensity to background ratio is improved. The atomic electron densities are better located in Fourier maps, because of the presence of higher order data and because they are confined to a smaller volume due to the reduction in the thermal motion. In this way, estimated standard deviations of the atomic coordinates will be lowered and more accurate bond lengths and angles can be derived. It is also evident that if less thermal motion means less smearing of the electron density, lowering the temperature will improve the chances of locating and properly characterising smaller features of the electron density. For example, it will increase the chances of locating and refining the positions of hydrogen atoms, which have only one electron contributing to the scattering of X-rays.

Moreover, as a consequence of the increase in intensity, lowering the temperature of the SXRD experiment will also allow the study of samples that at room temperature do not diffract X-rays strongly enough to be measured. In this way, reliable atomic positions can be obtained from samples that diffract too weakly, due to crystal size or dynamic disorder for example.

Another very neat application, which is nowadays probably used in more than 90% of small molecule SXRD low temperature experiments, is that of mounting the sample in a drop of oil.[27,28] This method basically consists of bathing a crystal in an inert oil (usually a perfluoropolyether) and attaching the crystal to a glass fibre, hair or fibre loop using the surface tension of the oil. The crystal is then flash frozen in a stream of cold nitrogen or helium gas together with the oil. The oil vitrifies, holding the crystal in place, and thus showing no Bragg diffraction, just a small contribution to the background scattering. Hence, speed is one of the primary advantages of this method, allowing fast screening of samples at low temperatures. Equally important however, covering the crystal with the oil protects samples from the environment, so it is used very frequently for the study of unstable or air/moisture sensitive compounds, as well as crystals prone to the loss of solvent. A final advantage of this cryocrystallographic method of mounting samples is that manipulation of the crystals in the oil causes them less physical damage and allows easier cutting and cleaning.

Once the sample is mounted at low temperature and in addition to, or even making use of, the benefits brought by the enhancement of intensity and data quality discussed above, the use of low temperature for SXRD has a number of traditional applications, which need a specific mention here.

Study of materials which are liquids or gases at room temperature

It is obvious that low temperature is needed in order to study materials in the crystalline state which are either liquids or gases at room temperature. The need for structural information on these types of materials has stimulated the development of specific methods for growing single-crystals '*in situ*', *e.g.* in the diffraction apparatus which will be used to perform these studies (a good review can be found in ref. 26). The basis of the technique involves cooling a liquid or a gas inside a capillary until they solidify. This will usually produce a polycrystalline sample. Warming up slowly will eventually melt these crystallites, although not all of them will melt together. The aim is to melt all but one crystallite, which will then become the seed of a crystal of the appropriate size for the diffraction experiment. This will be obtained by slow cooling of the sample, allowing the seed to grow and avoiding sudden precipitation of multiple crystallites. However, crystallisation by cooling often produces polycrystalline samples because nucleation occurs at lower temperatures than the melting point of the sample or the saturation point of the solution. In this respect, an important advance has been the use of an infrared laser for localised heating and melting of the sample in the capillary, which also avoids interference with the cold stream of gas from the low temperature device.[26] One of the advantages of growing a crystal on the diffractometer, is the possibility of observing the

crystallisation process by diffraction. The simplicity of this monitoring when using area detectors, with their speed to scan a large area of reciprocal space in one shot, has been vital to the rise in the number of studies making use of this technique in the last 10 years.

Charge density analyses

The use and progressive improvement in the use of low temperatures in SXRD have been linked traditionally to experiments performed to study the distribution of electrons in a material. The aim of a typical SXRD experiment is to find all atomic positions corresponding to the atoms forming a certain material, but these are obtained by considering atoms as spherical clouds of electrons. The positions of the atoms are then obtained by calculating the centroid of these electron clouds, as X-rays interact mainly with the electrons in atoms, and not with nuclei. It is natural therefore, if X-rays interact with electrons, that X-ray diffraction can be used to study the distribution of electrons within a material. However, this means that a diffraction experiment carried out with this purpose must look for finer details in a structure, *i.e.* the location of individual electrons and not just the atom as positioned in the centre of an electron cloud. As such, the experiment and the data thus obtained have to be of enhanced quality.

As mentioned before, lowering the temperature of the experiment will improve the quality of the data, by reducing TDS and anharmonicity and by increasing the intensity of the reflections, thus charge density experiments are best carried out at low temperatures. However, in addition to the benefits already mentioned, it is worth adding a few specific points to these types of studies. The reduction of thermal motion and as a consequence the reduction in the smearing of the electron density, not only permits the identification of small features of the electron density like hydrogen atoms, but also subtle features like the presence and location of lone pairs, the electron density participating in bonding, the electron density participating in intermolecular interactions, charge transfer between molecules and many more. Moreover, the reduction in thermal motion also enables the deconvolution of these features from the dynamic motion itself. As pointed out, the atomic displacement parameters will represent not only thermal motion, but also any static disorder or smearing of the electron density beyond the sphere representing an atom. For this reason, electron density located in preferential directions to bonding or other physical effects becomes masked by and confused with dynamic motion. Lowering the temperature of the experiment then makes it possible to deconvolute and analyse these different aspects of the behaviour of the electrons in a material. Furthermore, in these types of studies it is normal to refine up to thirty four parameters per atom (compared to the more usual nine that are refined in a typical crystal structure determination). So, the gain in intensity due to the low temperatures is needed in order to increase the number of observed reflections and thus provide a large enough number of observations per refined parameter to trust the results obtained. The gain in intensity will also be greater for high resolution data, and these data are the ones least influenced by the valence electrons. They contain mainly information on the core electrons and hence atomic positions and atomic displacement parameters obtained using these data are more reliable, and in fact they should be very similar to those obtained from neutron diffraction data, which rely on the interaction of neutrons with nuclei.[42–44] In spite of this, great care is needed when comparing quantities from different experiments. In particular, displacement parameters are very sensitive to small differences in temperature between experiments, as well as to systematic errors introduced by temperature dependent effects like anharmonicity and TDS.[43–45]

Phase transitions and thermal expansion coefficients

Low temperature crystallographic studies are essential in order to understand the reasons that a given material presents a particular chemical or physical property. Moreover, determining the crystal and molecular structures of a compound above and below a phase transition aids the understanding of the mechanisms controlling certain phase transitions and enables the correlation of structures with chemical and physical properties. Furthermore, following the changes in the values of unit cell parameters with temperature can lead to the detection of even very subtle phase transitions associated with changes in a material's properties, *e.g.* magnetic, optical, electric and so on. Low and multi-temperature experiments then enable the identification of the key elements that account for a given property and thus are the first step towards the design of new materials showing enhanced properties.

Another area in which this information proves very useful is in the study of materials that present negative thermal expansion, *i.e.* they expand on lowering the temperature.[46] There are a number of potential applications for this kind of material related to the possibility of producing composites that display a net zero coefficient of expansion over a wide range of temperatures, *e.g.* optical mirrors, fibre optics, cookware and also of manufacturing materials with tailored expansion coefficients that match those of another material, of importance in electronic and biomedical applications.

In addition, studying the influence that changes in temperature have on a crystal lattice is critical for materials intended for many practical applications. For example, the applications of non-linear optical materials usually involve subjecting a material to high-energy laser radiation. In these cases, the optical absorption induces thermal gradients within the crystal, and the nature and extent of the damage induced by the thermal contribution needs to be assessed. Possibilities include changes in unit cell parameters with temperature, as well as sample stress that can cause fractures.

Case studies

Multi-temperature structural study of a Cr(II) dinuclear complex

In 1994, Hughes *et al.*[47] reported a spin crossover transition on the triple decker dinuclear Cr(II) complex $[(\eta^5\text{–}C_5Me_5)\text{-}Cr(\mu^2\text{:}\eta^5\text{–}P_5)Cr(\eta^5\text{–}C_5Me_5)]^+$ $(SbF_6)^-$ (**TD**) at approximately 23 K (the cation is shown in Fig. 7). The sharpness of the transition, characteristic of cooperative behaviour, suggested that there could be a substantial structural change accompanying the magnetic transition. In order to shed light on the reasons for such behaviour, a careful multiple temperature structural study on this material was undertaken. A full report on the results of these experiments is in preparation,[48] but here we would like to highlight the effects that lowering the temperature of this compound has on the lattice parameters, the intensity of the data measured and the thermal motion.

Datasets were measured on a Bruker APEX CCD diffractometer equipped with an Oxford Cryostream[22] open flow N_2 gas and a Helix[40] open flow helium gas low temperature device. The former was used for unit cell measurements and data collections between 290 and 90 K (every 20 K), while the latter was used at 70, 50 and 30 K. In addition, data collections were carried out at 25 and 12 K (and unit cell measurements every 1 K between these two temperatures) using a 4-circle diffractometer equipped with a Displex Cryorefrigerator.[35]

Fig. 8(a) shows a plot of the volume of the unit cell of **TD** as a function of temperature. The structural changes that accompany the reported magnetic phase transition at 23 K can be clearly seen, as reflected in the unit cell volume. Moreover, although very subtle, the measurements show a change in the

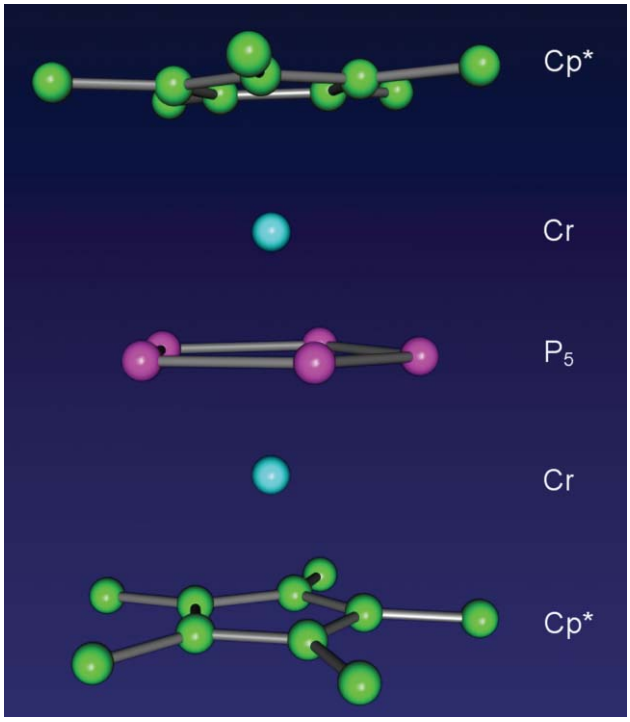

Fig. 7 Molecular structure of $[(\eta^5\text{–}C_5Me_5)Cr(\mu^2{:}\eta^5\text{–}P_5)Cr(\eta^5\text{–}C_5Me_5)]^+$, with the chromium atoms shown in cyan, phosphorus atoms in pink and carbon atoms in green.

slope of the volume contraction with temperature at 150 K. This is in complete agreement with the finding that there is a structural phase transition at this temperature, from the orthorhombic space group *Fddd* to the monoclinic *I*2/*a*, accompanying a change in the magnetic behaviour of **TD** at the same temperature, explained by Hughes *et al.*[47] as arising from the onset of an intramolecular antiferromagnetic interaction.

Fig. 8(b) shows the gain in intensity achieved by reducing the temperature of the experiment from 290 K to 90 K. At room temperature the material shows a dynamic disorder of the anions together with a librational disorder of the phosphorus ring. Lowering the temperature reduces both effects, improving not only the accuracy of all bond lengths (especially those involving the phosphorus atoms) but also resulting in a net increase in the intensity of the reflections, in particular those at high scattering angles. Fig. 9 shows how decreasing the temperature affects the thermal vibrations, as shown by the reduction in the average value of the equivalent isotropic displacement factors, U_{eq},[14] for the terminal carbon atoms of the Cp* rings and the phosphorus atoms of the P_5 ring. It is clear from this figure that the dynamic motion of the phosphorus atoms is larger than that of the methyl carbon atoms due to the librational disorder of the P_5 ring mentioned above. This is particularly emphasised above the phase transition at around 150 K.

In short, we can see from this example how carrying out measurements at lower temperatures not only allows us to follow the structural changes associated with a change in the physical properties of a material, but also shows how reducing the temperature of the experiment reduces the thermal vibrations, including librational disorder, and increases the intensity of the reflections.

Experimental study of the electron distribution in crystalline benzene

Benzene is the prototypical aromatic molecule and as such assumes a central role in the study of delocalised chemical

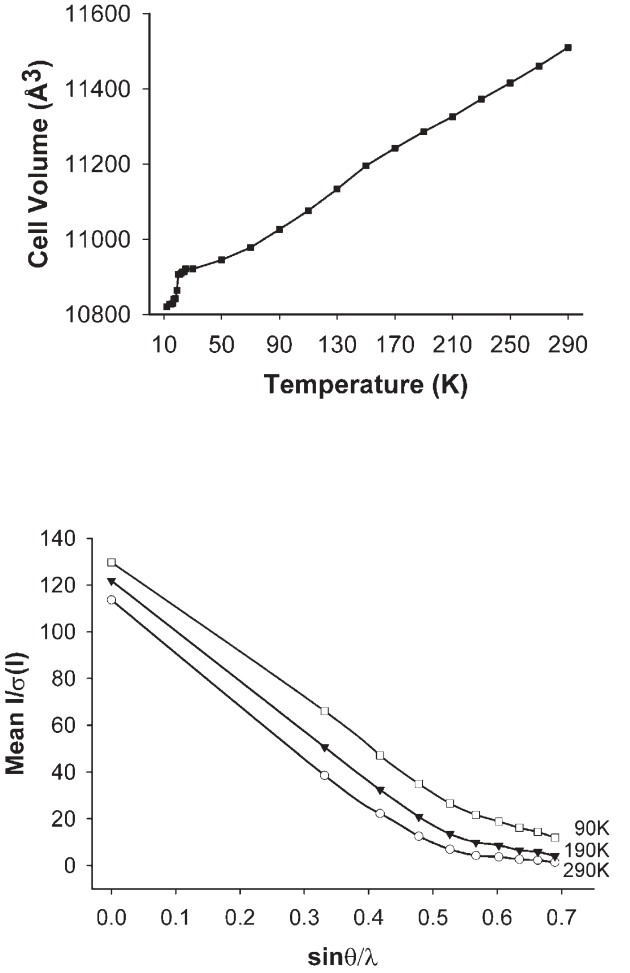

Fig. 8 (a) Unit cell volume of **TD** as a function of temperature between 290 K and 12 K, following the phase changes. (b) Mean intensity ($I/\sigma(I)$) of **TD** as a function of resolution ($\sin\theta/\lambda$) for data recorded at 290 K, 190 K and 90 K, showing the increase of $I/\sigma(I)$ on cooling.

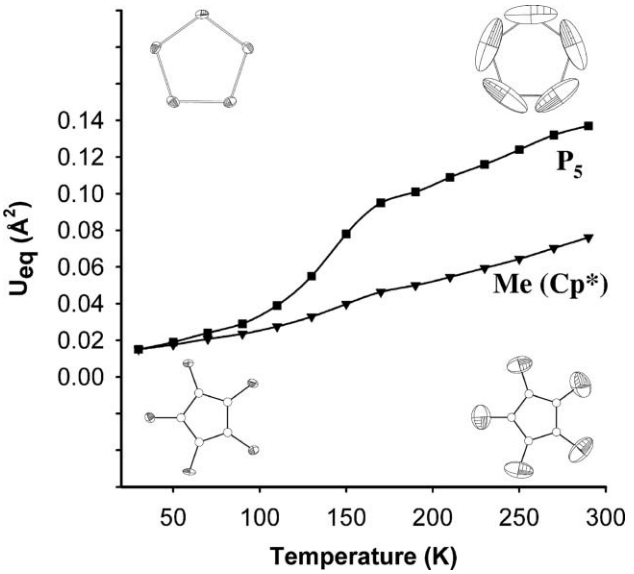

Fig. 9 Comparison of the mean equivalent isotropic displacement factors, U_{eq}, for the phosphorus atoms in the P_5 ring (affected by libration) and the terminal methyl carbon atoms of the Cp* groups as a function of temperature. Thermal ellipsoid plots are shown at 290 K and 30 K.

bonds and supramolecular interactions in the crystalline state. For this reason, detailed knowledge of the numerous electronic properties of benzene and its closely related derivatives is of fundamental importance in many areas of theoretical and experimental chemistry. In this context, the following work[42] was carried out with the aim of proving whether molecular properties of benzene, such as the molecular quadrupole moment and electric field gradients at hydrogen atoms (and hence deuterium quadrupole coupling tensors), could be obtained with an accuracy and precision comparable to that of other experimental techniques.

The need to use low temperatures for this and similar studies of the charge density and its properties has been highlighted above. However, in addition, the melting point of benzene is around 278 K (5 °C), making it necessary to use low temperatures for the crystallisation of the sample crystal '*in situ*' from its liquid form. Thus, a single crystal of benzene was grown in a 0.5 mm diameter glass capillary mounted on the goniometer of a Bruker SMART-1K CCD diffractometer equipped with an Oxford Cryostream open flow N_2 gas low temperature device.[22] A polycrystalline sample was obtained on cooling to 250 K, which was then warmed to 275 K until just a tiny crystalline seed remained in the very tip of the capillary. Slow cooling of the seed to 272 K produced a crystal of suitable quality. The crystal was then cooled further to 110 K for data collection.

An analytical representation of the electron distribution in the crystal, deconvoluted from the thermal motion of the atoms, was obtained by least-squares fitting of the measured intensities using the rigid pseudoatom model for multipole refinement of X-ray diffraction data.[49] This representation permits the clear visualisation of the bonding electron density that arises when isolated atoms gather together to form a molecule as shown by a map of the deformation electron density in benzene (Fig. 10). Distinguishing between features

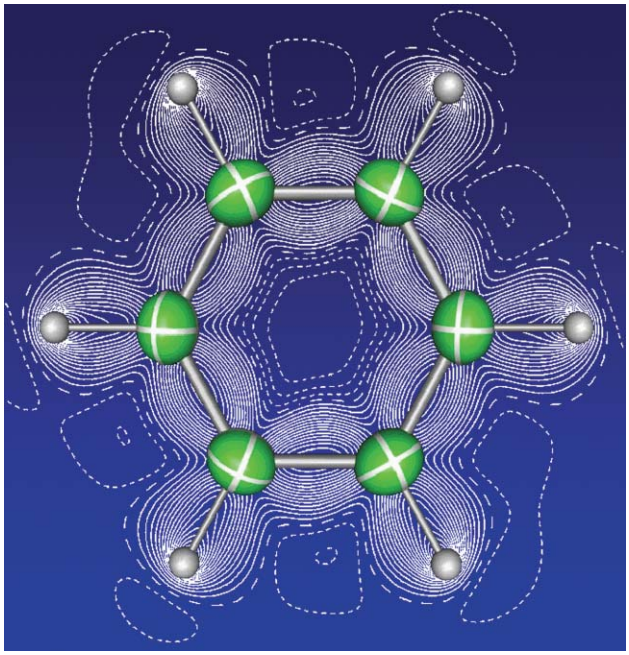

Fig. 10 Static deformation electron density in the molecular plane of benzene calculated as the multipole-derived electron density minus that of a superposition of spherical atoms. Contours at 0.05 eÅ^{-3} intervals; positive contours solid, zero and negative contours dashed.

arising from bonding and thermal motion is particularly important when seeking to obtain accurate values for properties, for example the molecular quadrupole moment. Hence, special efforts were undertaken to obtain an independent description of the thermal motion on C_6H_6 at the temperature of the X-ray experiment.[42]

The quality of the results obtained is usually first underlined by the final values of agreement factors, which in this case were very good indeed (for example $R(F^2) = 2.27\%$). In this example however, the quality of the final model describing the electron density distribution can also be assessed by the excellent agreement between the final values for the optimised radial exponents for the carbon and hydrogen atoms, with those found by Volkov *et al.*[50] from a detailed analysis of the multipole modelling of theoretical structure factors based on crystal density-functional calculations.

In addition, to achieve the aims that were the motivation for this work, values of the molecular quadrupole moment and the mean deuterium quadrupole coupling constant of the electric field gradient tensors at the H nuclei were calculated from the static electron distribution derived from the multipole refinement. Stressing even more the quality of the data and results, the multipole-derived value of the molecular quadrupole moment, $-29.7 \pm 2.4 \times 10^{40}$ C m, is of the same sign as, and lies both near and between independent measurements obtained in the gas phase and in dilute solution ($-30.4 \pm 1.2 \times 10^{40}$ C m and $-28.3 \pm 1.2 \times 10^{40}$ C m respectively).[51,52] A negative sign implies a ring of positive charge in the molecular plane near the hydrogen atoms, with negative regions above and below the ring. The value thus obtained from accurate low temperature measurements of high resolution X-ray diffraction is entirely consistent with the expectation that the weak intermolecular forces between the benzene molecules in the solid state have no observable effect on the molecular quadrupole moment. The value obtained for the mean deuterium quadrupole coupling constant (182 ± 17 KHz) is also in excellent agreement with values obtained from NQR experiments on single crystals and polycrystalline samples of C_6D_6.

These results clearly show that accurate X-ray diffraction data can be measured and that values for physical properties obtained from the analysis of the data are comparable to those obtained by other techniques. Moreover, within the context of this review, it is clear that the use of low temperature has been fundamental in order to achieve the goals of this work, not only due to the need for *in situ* crystallisation, but also for the deconvolution of the density associated with the thermal motion and bonding features, as well as for the general quality of the data collected.

Thermal and light induced spin transitions in spin-crossover complexes

Spin crossover (SCO) materials can reversibly change their magnetic spin states between a low temperature diamagnetic low-spin state (LS) and a high temperature paramagnetic high-spin state (HS). As well as different magnetic properties, the two spin states present different structural and optical properties which can be induced by changes in pressure or temperature. Moreover, in some cases the presence of abrupt thermal spin transitions and hysteresis confer to these materials a memory effect.[53] All these features have led to increasing interest in their potential use in technological applications such as molecular switches, data displays, data storage devices and more recently as intelligent contrast agents for magnetic resonance imaging.[54] Furthermore, the discovery that at low temperature it is sometimes possible to photo-excite SCO materials into a metastable high spin state[55] has opened up the possibility of these materials being used in optical devices and has enabled the study of high and low spin complexes without the added complication of thermal effects. The metastable high-spin states induced by this light-induced excited spin state trapping (LIESST) have been found to have very long lifetimes

at low temperatures with the highest reported LIESST temperature being 130 K.[56] However, while structural studies of thermally induced high and low spin complexes are increasingly common, structure determinations of the light induced metastable high spin state are still very rare, mainly for the need in most cases of temperatures below 77 K, with only a handful reported in the literature.[24,25,57]

The need for low temperatures to study the structural properties of these materials is evident, as structural studies of the different states are vital to fully understand the mechanisms driving the transitions. Moreover, the structural changes in each particular case need to be correlated with the magnetic changes, abruptness of the magnetic transitions, hysteresis, relaxation effects, *etc.* in order to help in designing new materials showing enhanced properties.

$[Fe(pmd)(H_2O)\{M(CN)_2\}_2]\cdot H_2O$ (pmd = pyrimidine; M = Ag or Au) is one of the latest examples of a thermal induced SCO material.[58] The material is a cyanide-based bimetallic coordination polymer made up of triple interpenetrated, three-dimensional, open-frame networks. The structure of this material shows two distinct iron atoms, Fe(1) and Fe(2), which define the inversion centre of one elongated $\{Fe(1)N_6\}$ octahedron and a compressed $\{Fe(2)N_4O_2\}$ coordination octahedron. In both cases the four equatorial positions are occupied by the cyanide nitrogen atoms of $[M(CN)_2]^-$ groups, while the apical positions are occupied by two nitrogen atoms of the two pmd ligands and by two water molecules (Fe(1) and Fe(2) respectively, see Fig. 11). Magnetic susceptibility

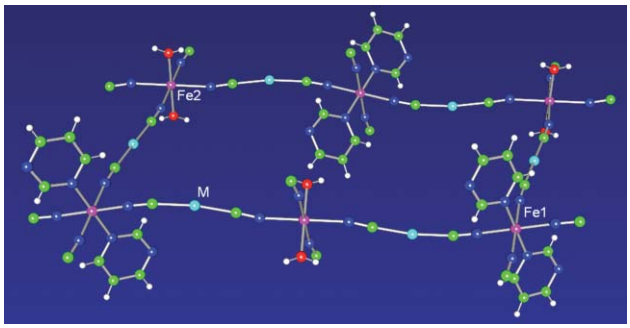

Fig. 11 Molecular structure of $[Fe(pmd)\text{–}(H_2O)\{M(CN)_2\}_2]\cdot H_2O$ showing how the $\{Fe(1)N_6\}$ and $\{Fe(2)N_4O_2\}$ octahedra are connected by $[M(CN)_2]^-$ ligands.

measurements carried out to monitor the SCO behaviour show that below the thermal transition temperature (around 219 K for the silver complex and 167 K for the gold complex), 50% of the iron(II) ions remain in the HS state. The structural data obtained at 120 K for both derivatives, *e.g.* average Fe–N distances, confirm that while Fe(1) undergoes the HS–LS transition, Fe(2) remains HS (Fe(1)–N = 1.95(3) Å and Fe(2)–N = 2.14(4) Å).

As mentioned above, crystal structure determinations of light induced high-spin states are very rare and one example is $[Fe(1,10\text{-phenanthroline})_2(NCS)_2]$.[25] The material undergoes an extremely abrupt thermal spin transition at 176 K, which may also occur at room temperature by applying pressure or at low temperature upon irradiation.[59] Single crystal X-ray diffraction was used to determine the crystal structure at 30 K, both in the low spin state and in the metastable high spin state (shown overlaid in Fig. 12), and to compare it with the crystal structure for the stable room-temperature high spin state.[59] X-Ray diffraction data at 30 K was obtained using an Oxford Cryosystems Helix open flow helium gas cryostat[40] mounted on a Bruker SMART-1K CCD area detector diffractometer (Fig. 6). After collecting data at 30 K on a sample in the

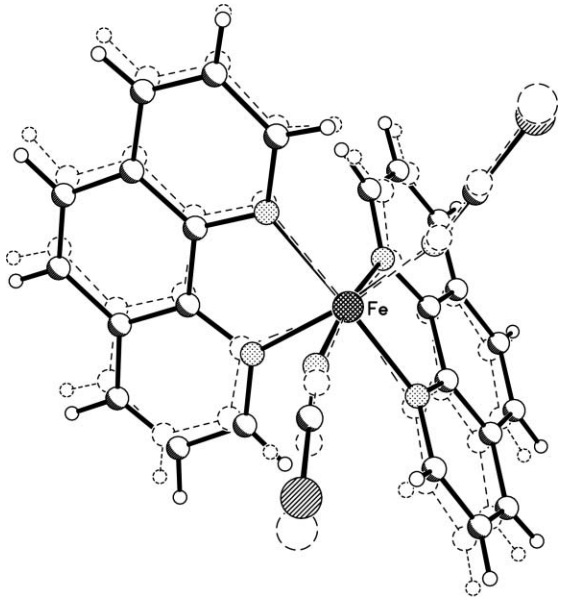

Fig. 12 Overlay of the low spin and metastable light induced high spin states of $[Fe(phen)_2(NCS)_2]$ at 30 K. The average Fe–N distance increases from 1.983(5) to 2.122(5) Å and the octahedron becomes more irregular on excitation from low spin to high spin.

low spin state, the same sample was irradiated with a He–Ne laser (λ = 647 nm, 5 mW cm^{-2}) for 1 h and diffraction data were immediately re-collected to determine the crystal structure of the metastable state. The LIESST temperature in this compound is around 60 K, so clearly temperatures lower than this value are required to study this photo-induced state. Moreover, the photoinduced HS–LS relaxation process needs to be slow enough to allow the data collection to be completed while the crystal is in the metastable state, and this is achieved at 30 K. An important result from this experiment concerns the decoupling of structural changes induced by thermal effects and those corresponding only to a change in the spin state. The low temperature X-ray data shows that the unit cell volume variation due to the light induced LS–HS transition is, in fact, very small (24 $Å^3$) and corresponds to an increase in the crystal volume of 1.1%. This change corresponds to the exact amplitude of the spin transition dilatation, while the volume variation (97 $Å^3$) between the room temperature HS state and the light induced HS state unit cells gives the amplitude of only the thermal contraction from 293 to 30 K. Studies of the crystal structures in both irradiated and non-irradiated states of a photoinduced molecular switch, like the one presented here and based on the spin-crossover phenomenon, bring relevant information not only for the study of the LIESST effect, but also in the general field of photoexcited states within the context of the design of new materials for electronic molecular devices. Once again, these studies are made possible by the use of low temperature crystallographic techniques.

Concluding remarks

Here we have shown the consequences and advantages of carrying out single crystal X-ray diffraction experiments at low temperatures, and hence the reasons behind low temperature SXRD becoming a standard procedure in modern university laboratories around the world. It has been demonstrated how the use of low temperature in SXRD experiments is essential for the understanding of chemical and physical properties of materials. The use of low temperature enables us to obtain detailed information on atomic displacements, electron density distributions, accurate geometrical parameters, structural changes accompanying phase transitions, the structure of

materials that are liquids or gases at room temperature, as well as many other significant aspects within chemistry. The advent of area detector systems has increased the feasibility of using more expensive cryogenic instrumentation and procedures, as well as performing multi-temperature data collections, by reducing the data acquisition time and therefore the cost of the experiment. This has enhanced even more the significance of using low temperatures to derive structure-property correlations, as demonstrated by the examples presented herein. In addition, the development of new, low temperature instrumentation in the past five years has increased both the interest in and the availability of low temperature SXRD, also making such studies more economical. Within this context, it is foreseeable that low temperature SXRD will become even more common, accessible and important to the scientific community. As such, it is vital that the consequences, advantages and applications of low temperatures for structural studies are neither forgotten, nor forgotten to be learnt.

References

1 F. H. Allen, O. Kennard and R. Taylor, *Acc. Chem. Res.*, 1983, **16**, 146.
2 F. K. Larsen, *Acta Crystallogr.*, 1995, **B51**, 468.
3 F. K. Larsen, in *The Application of Charge Density Research to Chemistry and Drug Design.*, ed. G. A. Jeffrey and J. F. Piniella, Plenum Press, New York, 1991.
4 C. C. F. Blake and D. C. Philips, *Biological Effects of Ionizing Radiation at the Molecular Level*, Symposium of the International Atomic Energy Agency, Vienna, Austria, 1962, p. 183.
5 S. C. Abrahams, *Acta Crystallogr., Sect. A*, 1973, **29**, 111.
6 *International Tables for Crystallography*, ed. A. J. C. Wilson, Kluwer Academic Publishers, Dordrecht/Boston/London, 1992, **vol. C**, p. 168 and references therein.
7 P. Seiler and J. D. Dunitz, *Aust. J. Phys.*, 1985, **38**, 405.
8 E. F. Garman and T. R. Schneider, *J. Appl. Crystallogr.*, 1997, **30**, 211 and references therein.
9 A. Gonzalez, A. Thompson and C. Nave, *Rev. Sci. Instrum.*, 1992, **63**, 1177.
10 A. Gonzalez and C. Nave, *Acta Crystallogr., Sect. D*, 1994, **50**, 874.
11 C. Nave, *Radiat. Phys. Chem.*, 1995, **45**(3), 483.
12 R. Henderson, *Proc. R. Soc. London, Ser. B*, 1990, **241**, 6.
13 W. P. Burmeister, *Acta Crystallogr., Sect. D*, 2000, **56**, 328 and references therein.
14 J. P. Glusker, M. Lewis and M. Rossi, *Crystal Structure Analysis for Chemists and Biologists*, VCH Publishers, New York/Weinheim/Cambridge, 1994 and references therein.
15 *International Tables for Crystallography*, ed. C. H. Macgillavry, G. D. Rieck and K. Lonsdale, D. Reidel Publishing Company, Dordrecht/Boston/Lancaster/Tokyo, 1985, **vol. III**.
16 B. N. Figgis, L. Khor, E. S. Kucharski and P. A. Reynolds, *Acta Crystallogr., Sect. B*, 1992, **48**, 144.
17 B. T. M. Willis and A. W. Pryor, *Thermal Vibrations in Crystallography*, Cambridge University Press, Cambridge, Great Britain, 1975.
18 J. Dam, S. Harkema and D. Feil, *Acta Crystallogr., Sect. B*, 1983, **39**, 760.
19 B. B. Iversen, S. K. Nielsen and F. K. Larsen, *Philos. Mag. A*, 1995, **72**, 1357.
20 R. Rudman, *Low Temperature X-ray Diffraction, Apparatus and Techniques*, Plenum Press, New York and London, 1976.
21 R. Rudman, H. Hope, E. D. Stevens and G. A. Petsko, *LTXRD Tutorial*, Asilomar, California, American Crystallographic Association publication, 1977.
22 J. Cosier and A. M. Glazer, *J. Appl. Crystallogr.*, 1986, **19**, 105.
23 S. J. Reeuwijk, A. Puig-Molina and H. Graafsma, *Phys. Rev. B*, 2001, **64**, 134105.
24 V. A. Money, I. R. Evans, M. A. Halcrow, A. E. Goeta and J. A. K. Howard, *Chem. Commun.*, 2003, 158.
25 M. Marchivie, P. Guionneau, J. A. K. Howard, G. Chastanet, J.-F. Létard, A. E. Goeta and D. Chasseau, *J. Am. Chem. Soc.*, 2002, **124**, 194.
26 R. Boese and M. Nussbaumer, *In situ* Crystallization Techniques, in *Correlations, Transformations and Interactions in Organic Crystal Chemistry, IUCr Crystallographic Symposia*, ed. D. W. Jones and A. Katrusiak, Oxford University Press, Oxford, England, 1994, **vol. 7**, pp. 20–37.
27 T. Kottke and D. Stalke, *J. Appl. Crystallogr.*, 1993, **26**, 615.
28 H. Hope, *Acta Crystallogr., Sect. B*, 1988, **44**, 22.
29 M. J. Hardie, K. Kirschbaum, A. Martin and A. A. Pinkerton, *J. Appl. Crystallogr.*, 1998, **31**, 815.
30 L. Ribaud, G. Wu, Y. Zhang and P. Coppens, *J. Appl. Crystallogr.*, 2001, **34**, 76.
31 See for example: http://www.oxford-diffraction.com/helijet.htm and http://www.cryoindustries.com/crystal.htm.
32 P. Coppens, F. K. Ross, R. H. Blessing, W. F. Cooper, F. K. Larsen, J. G. Leipoldt, B. Rees and R. Leonard, *J. Appl. Crystallogr.*, 1974, **7**, 315.
33 K. Henriksen, F. K. Larsen and S. E. Rasmussen, *J. Appl. Crystallogr.*, 1986, **19**, 390.
34 D. Zobel, P. Luger, W. Dreissig and T. Koritsanszky, *Acta Crystallogr., Sect. B*, 1992, **48**, 837.
35 R. C. B. Copley, A. E. Goeta, C. W. Lehmann, J. C. Cole, D. S. Yufit, J. A. K. Howard and J. M. Archer, *J. Appl. Crystallogr.*, 1997, **30**, 413.
36 See for example: http://harker.chem.buffalo.edu, http://www.dcfe.unimi.it/destro.htm, http://www.lks.physik.uni-erlangen.de and http://www.physics.helsinki.fi/~xray_www.
37 For more information contact: AS Scientific Products Ltd., 2 Barton Lane, Abingdon Science Park, Abingdon, Oxon OX14 3NB or Advanced Research Systems Inc., 905 Harrison Street #109, Allentown, PA 18103, USA.
38 A. E. Goeta, L. K. Thompson, C. L. Sheppard, S. S. Tandon, C. W. Lehmann, J. Cosier, C. Webster and J. A. K. Howard, *Acta Crystallogr., Sect. C*, 1999, **55**, 1243.
39 M. A. Leech, N. K. Solanki, M. A. Halcrow, J. A. K. Howard and S. Dahaoui, *Chem. Commun.*, 1999, 2245.
40 Oxford Cryosystems Newsletter, July 2003.
41 Oxford Cryosystems Newsletter, February 2004.
42 H. B. Bürgi, S. C. Capelli, A. E. Goeta, J. A. K. Howard, M. A. Spackman and D. S. Yufit, *Chem.–Eur. J.*, 2002, **8**, 3512.
43 B. N. Figgis, B. B. Iversen, F. K. Larsen and P. A. Reynolds, *Acta Crystallogr., Sect. B*, 1993, **49**, 794.
44 B. B. Iversen, F. K. Larsen, B. N. Figgis, P. A. Reynolds and A. J. Schultz, *Acta Crystallogr., Sect. B*, 1996, **52**, 923.
45 P. Coppens and A. Vos, *Acta Crystallogr., Sect. B*, 1971, **27**, 146.
46 J. S. O. Evans, *J. Chem. Soc., Dalton Trans.*, 1999, 3317.
47 A. K. Hughes, V. J. Murphy and D. O'Hare, *J. Chem. Soc., Chem. Commun.*, 1994, 163.
48 A. E. Goeta, R. C. B. Copley, J. A. K. Howard, A. K. Hughes and D. O'Hare, manuscript in preparation.
49 P. Coppens, *X-Ray Charge Densities and Chemical Bonding*, Oxford University Press, New York, 1997.
50 A. Volkov, Y. A. Abramov and P. Coppens, *Acta Crystallogr., Sect. A*, 2001, **57**, 272.
51 G. L. D. Ritchie and J. N. Watson, *Chem. Phys. Lett.*, 2000, **322**, 143.
52 G. R. Dennis and G. L. D. Ritchie, *J. Phys. Chem.*, 1991, **95**, 656.
53 P. Gütlich, A. Hauser and H. Spiering, *Angew. Chem., Int. Ed. Engl.*, 1994, **33**, 2024 and references therein.
54 O. Kahn and C. J. Martinez, *Science*, 1998, **279**, 44.
55 S. Decurtins, P. Gütlich, K. M. Hasselbach, H. Spiering and A. Hauser, *Inorg. Chem.*, 1985, **24**, 2174.
56 S. Hayami, Z. Gu, Y. Einaga, Y. Kobayasi, Y. Ishikawa, Y. Yamada, A. Fujishima and O. Sato, *Inorg. Chem.*, 2001, **40**, 3240.
57 A. L. Thompson, PhD Thesis, University of Durham, 2004 and references therein.
58 V. Niel, A. L. Thompson, M. Carmen Muñoz, A. Galet, A. E. Goeta and J. A. Real, *Angew. Chem., Int. Ed.*, 2003, **42**, 3760.
59 B. Gallois, J. A. Real, C. Hauw and J. Zarembovitch, *Inorg. Chem.*, 1990, **29**, 1152 and references therein.